Stepwise Sequential and Parallel Photoinduced Charge Separation in a Porphyrin−Triquinone Tetrad†

Joseph Springer, Gerdenis Kodis, Linda de la Garza, Ana L. Moore,* Thomas A. Moore,* and Devens Gust*

Department of Chemistry and Biochemistry, Center for the Study of Early Events in Photosynthesis, Arizona State University, Tempe, Arizona 85287

Received: November 13, 2002; In Final Form: February 11, 2003

A molecular tetrad consisting of a free base porphyrin (P) linked to a triquinone moiety consisting of a naphthoquinone bearing two benzoquinones ($NQ-BQ_2$) has been synthesized and its photochemistry has been investigated using time-resolved spectroscopic techniques. Excitation of the porphyrin chromophore of the $P-NQ-BQ_2$ tetrad in benzonitrile solution is followed by photoinduced electron transfer with a rate constant of 8.3×10^{10} s^{-1} to produce an initial $P^{\bullet+}-NQ^{\bullet-}-BQ_2$ state with a quantum yield of unity. A charge shift reaction gives a final $P^{\bullet+}-NQ-(BQ^{\bullet-}BQ)$ charge-separated state, which decays to the ground state with a rate constant of 1.9×10^{10} s^{-1}. The tetrad features both sequential and parallel multistep electron-transfer pathways. No evidence was found for significant involvement of direct electron transfer from the porphyrin first excited singlet state to a benzoquinone.

Introduction

A key feature of photosynthetic energy conversion is photoinduced electron transfer to generate an energetic, long-lived charge-separated state in high quantum yield. The long lifetime is achieved by production of a final charge-separated state in which the electronic coupling between the radical ions is weak. Formation of this state with a high quantum yield is accomplished using a multistep pathway whereby electrons migrate from the excited primary donor to the final acceptor by sequential transfer via a number of intermediate donor/acceptor moieties. The electronic coupling for each intermediate electron "hop" is relatively large, so that transfer is rapid and efficient.

Many photosynthetic models using porphyrins or related cyclic tetrapyrroles as donor chromophores covalently linked to various organic species that act as electron acceptors and secondary donors have been reported.[1−10] Quinones are often used as electron acceptor species and indeed are among the acceptors found in natural photosynthetic electron transport. Although the majority of such models contain only a single quinone as an electron acceptor, some contain multiple quinones. For example, porphyrins linked to diquinones of sequentially increasing reduction potential demonstrate two sequential electron-transfer steps leading to an enhancement of the lifetime of charge separation.[3,11−13] On the other hand, a porphyrin−diquinone triad was recently reported in which both quinone moieties were of similar reduction potential.[14] The porphyrin was covalently linked to a benzoquinone derivative, which in turn bore a second benzoquinone. It was reported that the porphyrin first excited singlet state was quenched by direct photoinduced electron transfer both to the directly attached benzoquinone and to the additional benzoquinone moiety. Sequential electron transfer was not detected, even when such a pathway was thermodynamically feasible.

Herein we report the synthesis and spectroscopic study of tetrad **1**, in which a porphyrin (P) is joined to a naphthoquinone (NQ) via an amide linkage. The naphthoquinone in turn bears two equivalent benzoquinone moieties (BQ). This molecule has the potential for demonstrating sequential photoinduced electron transfer in addition to single-step transfer to the naphthoquinone and/or benzoquinones. In the first step, the porphyrin first excited singlet state, $^1P-NQ-BQ_2$, could in principle decay to initial charge-separated states $P^{\bullet+}-NQ^{\bullet-}-BQ_2$ or $P^{\bullet+}-NQ-(BQ^{\bullet-}BQ)$. Because the benzoquinones are more easily reduced than the naphthoquinone, charge shift from $P^{\bullet+}-NQ^{\bullet-}-BQ_2$ to yield $P^{\bullet+}-NQ-(BQ^{\bullet-}BQ)$ is a possibility. The resulting state could have a longer lifetime than $P^{\bullet+}-NQ^{\bullet-}-BQ_2$, due to reduced electronic coupling of the radical ions. In addition, the yield of $P^{\bullet+}-NQ-(BQ^{\bullet-}BQ)$ could be higher than that for a similar system having only one benzoquinone because two electron-transfer pathways acting in parallel would compete with decay of the precursor state. Finally, having two identical benzoquinones as the ultimate electron acceptors might permit construction of a donor−acceptor system capable of demonstrating accumulation of multiple reducing and oxidizing equivalents following multiple excitations. Tetrad **1** was prepared to investigate these possibilities and to compare its behavior with the earlier diquinone systems mentioned above.

Synthesis

The synthetic route to **1** and related model compounds is shown in Scheme 1. The triptycene derivative **6**, bearing the three quinones protected as dimethoxybenzene and dimethoxynaphthalene moieties, was prepared using the Diels−Alder reaction of the appropriate naphthoquinone with 1,4,5,8-tetramethoxyanthracene. Molecule **6** was linked to aminoporphyrin **10** through amide formation to yield **7**, and the protecting groups were removed to generate tetrad **1**. Dyad **2**, in which the two benzoquinone moieties have been reduced and protected as dimethoxybenzene derivatives, was prepared by a

† Part of the special issue "George S. Hammond & Michael Kasha Festschrift".

10.1021/jp022424g CCC: $25.00
Published on Web 03/27/2003

SCHEME 1

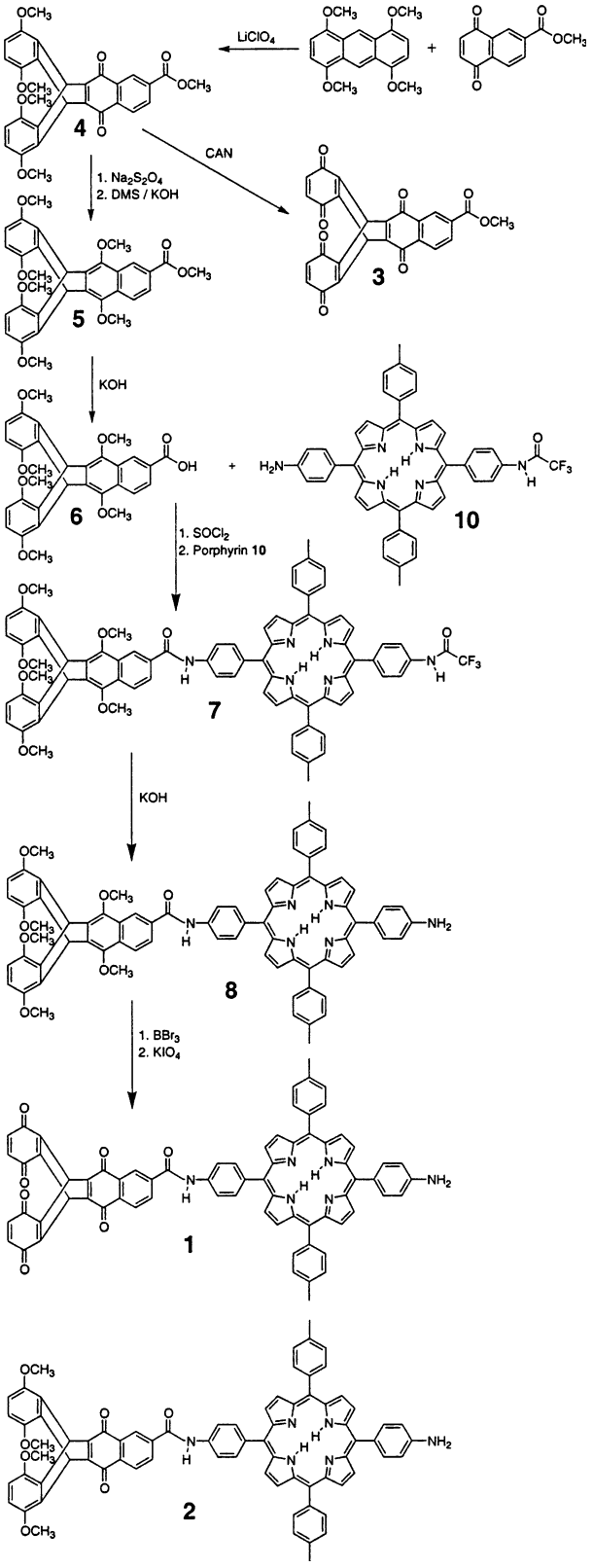

similar method. Details of the syntheses and characterization information are given in the Experimental Section.

Electrochemical and Spectroscopic Results

Cyclic Voltammetry. Electrochemical studies of model compounds were undertaken to derive estimates for the energies of the various charge-separated states that might be formed upon excitation of the donor−acceptor molecules. Measurements were carried out with a glassy carbon working electrode, a Ag/Ag^+ reference electrode, and a platinum counter electrode. The benzonitrile solutions contained the electrolyte 0.1 M tetra-*n*-butylammonium hexafluorophosphate, and ferrocene as an internal redox system. The results are listed in Table 1.

TABLE 1: Electrochemical Reduction Potentials for Quinones, vs SCE

compound	R_1	R_2	R_3
3	−0.29[a]	−0.47[a]	−0.71[a]
4	−0.52[a]		
12	−0.37[b], −0.46[c], −0.46[a]		
13	−0.23[b]	−0.48[b]	
14	−0.47[c]		

[a] Measured by cyclic voltammetry in benzonitrile, as described in the text. R_1 represents reduction of a benzoquinone moiety. [b] Measured $E_{1/2}$ in dimethylformamide.[19] [c] Measured by dc polarography in acetonitrile.[20]

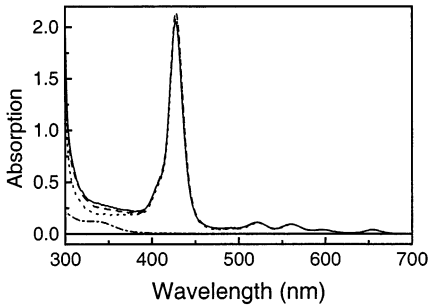

Figure 1. Absorption spectra in benzonitrile of tetrad **1** (—), dyad **2** (— — —), model porphyrin **11** (···), and model triquinone **3** (—·—). The spectra for **1**, **2**, and **11** have been normalized at the Q-band at ∼650 nm.

Model naphthoquinone **4** had a first reduction potential of −0.52 V vs SCE. For triquinone **3**, reduction potentials of −0.29, −0.47, and −0.71 V were determined. A model for the porphyrin moiety of **1** and **2**, 5,15-bis(4-acetamidophenyl)-10,20-bis(4-methylphenyl)porphyrin, has a first oxidation potential in benzonitrile of +0.93 V vs SCE.[15]

Absorption Spectra. Figure 1 shows the absorption spectrum of porphyrin−triquinone tetrad **1** in benzonitrile, along with the spectra of a model porphyrin, 5-(4-acetamidophenyl)-15-(4-aminophenyl)-10,20-bis(4-methylphenyl)porphyrin (**11**) and model triquinone **3**. The spectrum of model porphyrin **11** has maxima at 428, 522, 561, 598 and 655 nm. Dyad **2** and tetrad **1** have absorption maxima at 426, 521, 559, 596, and 653 nm. These maxima are ascribed to the porphyrin Soret (426−428 nm) and Q-bands. Spectra in chloroform, 2-methyltetrahydrofuran, and dichloromethane are similar, with shifts of absorption maxima ≤6 nm. The absorption features below 400 nm are due mainly to the quinone moieties. Triquinone model **3** has maxima at 239, 280 (shoulder), and 335 nm. The spectra of tetrad **1** and dyad **2** are similar to linear combinations of those of the model compounds, indicating the absence of strong electronic interactions between the moieties.

Fluorescence Emission. The fluorescence spectrum of model porphyrin **11** in benzonitrile with excitation at 590 nm is typical of free-base tetraarylporphyrins, featuring maxima at 666 and 730 nm in the intensity ratio 1.9:1 (Figure 2).The spectra of tetrad **1** and dyad **2** have similar shapes, but with maxima at 662 and 727 nm. Emission from these two compounds is strongly quenched, relative to that of **11**. By analogy with a very large number of other porphyrin−quinone conjugates, this quenching is ascribed to photoinduced electron transfer to

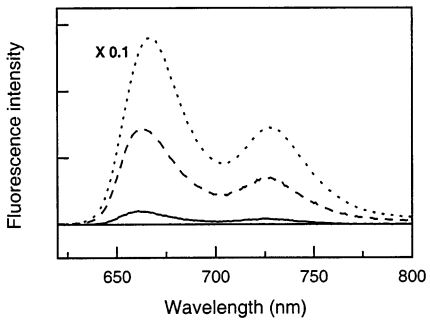

Figure 2. Fluorescence emission spectra of ~1 × 10^{-5} M solutions of tetrad **1** (—), dyad **2** (− − −), and model porphyrin **11** (···) in benzonitrile following excitation at 590 nm. The absorbances of the samples at the excitation wavelength were identical, and the spectrum of **11** has been multiplied by 0.1. The spectra have been corrected for the wavelength dependence of the detection system.

produce charge-separated states consisting of biradicals containing the porphyrin radical cation and quinone radical anion. Interpreting steady-state quenching data in terms of rate constants in such systems is risky because small amounts of unquenched porphyrin (e.g., from molecules in which the quinones have been reduced to hydroquinones by adventitious impurities) can introduce large errors. We therefore turned to time-resolved techniques to obtain more reliable information.

Time-Resolved Fluorescence. Time-resolved fluorescence experiments were performed using the single-photon-timing technique. Solutions of model porphyrin **11**, tetrad **1**, and dyad **2** in benzonitrile were excited at 590 nm, and the fluorescence decays were measured at 650 nm. Analysis of the model porphyrin data yielded a single-exponential decay with a lifetime of 9.9 ns (χ^2 = 1.13). The data for tetrad **1** were fitted satisfactorily by three exponentials (χ^2 = 1.01). There was one major decay component with a lifetime of 12 ps. Additional, minor components with lifetimes of 0.066 ns (9%) and 3.0 ns (0.6%) are ascribed to impurities. The data for dyad **2** also required three exponentials (χ^2 = 1.12): a major, 42-ps component and two minor components with lifetimes of 190 ps (4%) and 9.9 ns (5%).

In dichloromethane, the first excited singlet state of model porphyrin **11** decayed as a single exponential (χ^2 = 1.14) with a lifetime of 7.8 ns. The data for tetrad **1** were fitted as four exponential decays (χ^2 = 1.11) with lifetimes of ~6 ps (97%), 88 ps (2%), 1.5 ns (0.2%), and 7.8 ns (0.4%). The lifetime of 6 ps is close to the response capabilities of the apparatus, and therefore less certain than the other values. For dyad **2**, a three-exponential fit (χ^2 = 1.20) gave lifetimes of 30 ps (93%), 180 ps (3%), and 7.8 ns (4%).

Time-Resolved Absorption. Transient absorption measurements on ultrashort time scales were undertaken to study nonemissive transient species such as charge-separated states. Solutions of **1** and **2** in benzonitrile were excited with ~100-fs laser pulses, and transient spectra were recorded using the pump−probe method. The spectra were measured in the 450−775 nm region, at times ranging from −50 to +4500 ps relative to the laser flash. The data were fitted as sums of exponential components using global analysis and singular value decomposition methods. Typical spectra and time responses are shown in Figure 3.

Results for dyad **2**, with excitation at 555 nm, are shown in Figure 3a. The spectra at all times generally resemble those of the porphyrin first excited singlet state, although there is some spectral evolution with time. The inset shows that at 723 nm, there is a grow-in of a transient absorbance with a time constant

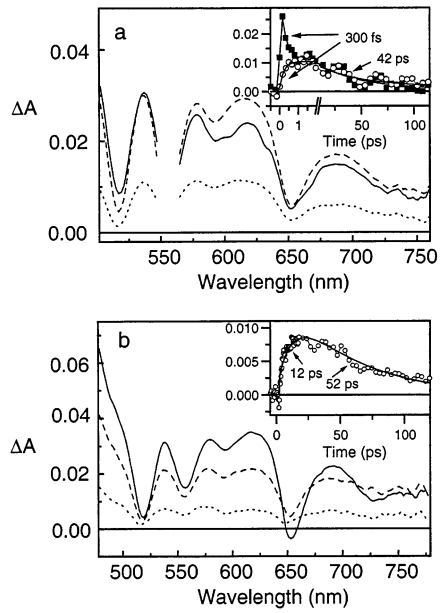

Figure 3. Transient absorption spectra of benzonitrile solutions of tetrad **1** and dyad **2** following excitation with ~100 fs laser pulses. (a) Spectra for dyad **2** taken 0.5 ps (—), 1.3 ps (− − −), and 60 ps (···) after excitation with a laser pulse at 550 nm. The inset shows the rise and decay of the transient absorbance at 510 nm (■) and 723 nm (○). The smooth lines in the inset are exponential fits to the data with time constants of 300 fs and 42 ps. (b) Spectra for tetrad **1** taken 3 ps (—), 20 ps (− − −), and 75 ps (···) after excitation with a laser pulse at 650 nm. The inset shows the rise and decay of the transient absorbance at 660 nm. The smooth lines are exponential fits to the data with time constants of 12 and 52 ps.

of 300 fs, followed by a slower decay of the spectral feature with a time constant of 42 ps. At 510 nm, there is prompt formation of a transient absorption that decays biexponentially with time constants of 300 fs and 42 ps. No longer-lived transients were detected.

Results for tetrad **1** with porphyrin excitation at 650 nm appear in Figure 3b. The spectrum at 3 ps consists mainly of features attributable to the porphyrin first excited singlet state. The broad absorption of the excited state is punctuated by negative features corresponding to bleaching of the Q-bands (see Figure 1). In addition, porphyrin stimulated emission (due to the probe pulse) is seen at ~650 and ~725 nm. At longer times, stimulated emission is no longer observed, and the spectra are characteristic of the porphyrin radical cation, which has a broad, rather featureless band in this spectral region.[16] The inset in Figure 3b shows the growth and decay of the transient absorption at 660 nm. The growth represents the disappearance of the porphyrin first excited singlet state and the formation of the porphyrin radical cation, whereas the decay tracks the disappearance of the radical cation. Measurements at a variety of wavelengths show that the time constant for formation of the porphyrin radical cation is 12 ps, and its lifetime is 52 ps.

Discussion

Photoinduced Electron Transfer. The transient absorption and emission data for **1** and **2** in benzonitrile can be interpreted in terms of decay of the porphyrin first excited singlet state by photoinduced electron transfer to a quinone to generate a charge-separated state. We will begin by discussing the results for dyad **2**. The transient absorption data reveal that excitation forms a transient with a lifetime of 42 ps that has spectral characteristics close to those of the porphyrin first excited singlet state. This

TABLE 2: Thermodynamic Driving Force and Rate Constant Values for Electron-Transfer Reactions of Triad 1 and Dyad 2

	photoinduced electron transfer		charge recombination	
compound	$\Delta G°$ (eV)	$10^{-10}k_{ET}$ (s^{-1})	$\Delta G°$ (eV)	$10^{-10}k_{CR}$ (s^{-1})
triad **1**	≤ -0.58[a]	8.3 (k_2)	−1.22	1.9 (k_6)
dyad **2**	−0.44	2.4 (k_2)	−1.45	∼300 (k_3)

[a] Estimated as described in the text.

finding is in accord with the time-resolved fluorescence data, which also indicate a lifetime of 42 ps for ^{1}P−NQ. The transient absorption data (Figure 3a) verify these conclusions but also reveal a rise time of ∼300 fs for the absorbance at 723 nm. Although one might be tempted to attribute this to the formation of the excited singlet state with the laser pulse, this is not the case. At 510 nm, the prompt formation of the porphyrin first excited singlet state (giving rise to $S_1 \rightarrow S_n$ absorption) is followed by a two-component exponential decay. The short decay component also has a ∼300 fs lifetime. To what can this kinetic component be attributed? Transient absorption and emission studies of several closely related porphyrin−quinone dyads[15,17] have revealed that recombination of $P^{\bullet+}-Q^{\bullet-}$ charge-separated states in these systems is significantly more rapid that their formation by photoinduced electron transfer. This leads to "inverted kinetic" behavior where the rise time of the transient absorbance correlates with the recombination of $P^{\bullet+}-Q^{\bullet-}$, and the decay represents the formation of the charge-separated state. Given the similar behavior for **2**, we assign the 42 ps time constant to formation of $P^{\bullet+}-NQ^{\bullet-}$ from ^{1}P−NQ. The decay of $P^{\bullet+}-NQ^{\bullet-}$ to the ground state by charge recombination is associated with the ∼300 fs time constant.

The rate constant for photoinduced electron transfer, k_{ET}, in dyad **2** is given by

$$k_{ET} = \frac{1}{\tau} - \frac{1}{\tau_0} \quad (1)$$

where τ is the 42 ps lifetime of the porphyrin first excited singlet state in dyad **2** and τ_0 is the lifetime of the excited singlet state in the absence of the electron-transfer process. The value for τ_0 may be estimated as 9.9 ns, on the basis of the fluorescence lifetime of model porphyrin **11**. Thus, $k_{ET} = 2.4 \times 10^{10}$ s^{-1} (Table 2). The quantum yield of electron transfer, Φ_{ET}, may be calculated from

$$\Phi_{ET} = k_{ET}\tau \quad (2)$$

and equals 1.0. The rate constant for charge recombination of $P^{\bullet+}-NQ^{\bullet-}$ is $\sim 3 \times 10^{12}$ s^{-1}.

Turning now to tetrad **1**, the time-resolved fluorescence data indicate a lifetime for ^{1}P−NQ−BQ_2 of 12 ps, and the same time constant for the decay of the porphyrin first excited singlet state and concurrent formation of the charge-separated state was observed by transient absorption. The longer-lived (52 ps) transient absorption is assigned to the decay of a charge-separated state, and inverted kinetics are not involved. What is the nature of the charge-separated state, $P^{\bullet+}-NQ^{\bullet-}-BQ_2$ or $P^{\bullet+}-NQ-(BQ^{\bullet-}BQ)$? The spectral signatures of the quinone radical anions appear in a congested region of the spectrum, are small, and cannot be differentiated in our experiment. However, given the structural similarity between **1** and **2**, and the fact that the lifetime of $P^{\bullet+}-NQ^{\bullet-}$ in **2** is ∼300 fs, we conclude that the transient absorbance is due to the $P^{\bullet+}-NQ-(BQ^{\bullet-}BQ)$ charge-separated state. The weaker electronic coupling between the radical ions is expected to slow recombination of $P^{\bullet+}-NQ-(BQ^{\bullet-}BQ)$. Using the formulas in eqs 1 and 2, we calculate a k_{ET} value of 8.3×10^{10} s^{-1} for **1**, and a quantum yield for charge separation of 1.0. The rate constant for charge recombination, k_{CR}, is 1.9×10^{10} s^{-1} (Table 2).

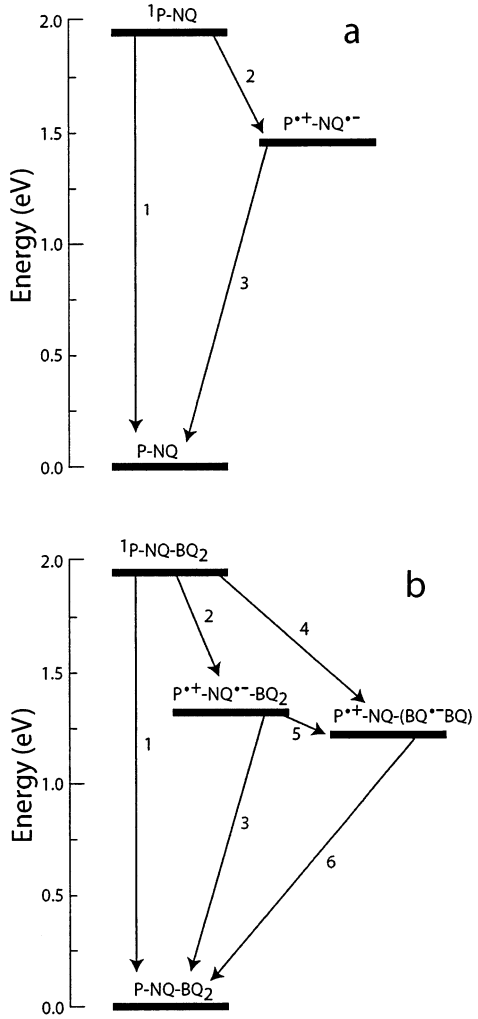

Figure 4. Transient species and relevant interconversion pathways in benzonitrile for (a) P−NQ dyad **2** and (b) P−NQ−BQ_2 tetrad **1**.

Energetics. Figure 4a shows the transient states that might be formed upon excitation of the porphyrin moiety of dyad **2** and interconversion pathways. The energy of the porphyrin first excited singlet state, 1.89 eV, is determined from the wavenumber average of the longest wavelength absorption maximum and the shortest wavelength emission maximum. The energy of the $P^{\bullet+}-NQ^{\bullet-}$ charge-separated state is estimated as 1.45 eV, on the basis of the electrochemical potentials given above. No attempt to correct this energy for Coulombic effects in the charge-separated state has been made.

A similar scheme for tetrad **1** is shown in Figure 4b. The porphyrin first excited singlet state lies 1.89 eV and the $P^{\bullet+}-NQ-(BQ^{\bullet-}BQ)$ state 1.22 eV above the ground state, on the basis of the first oxidation potential of the model porphyrin, mentioned above, and the first reduction potential of model triquinone **3** (Table 1). Estimating the energy of $P^{\bullet+}-NQ^{\bullet-}-BQ_2$ is more difficult. Direct electrochemical measurements of the reduction of the naphthoquinone moiety of **1** or of model system **3** are impossible because cyclic voltammetric reduction of the naphthoquinone can occur only following the initial reduction of the benzoquinones at higher potential. The reduction potential of the naphthoquinone in this case is lowered relative

to that in the neutral molecule due to the negative charges already present. Although one might be tempted to make an estimation on the basis of the first reduction potential of model quinone **4** (−0.52 V), this would not be correct. It is well-known that the three π-electron systems found in triptycene and related structures are able to interact electronically. Studies of triptycene-based quinones, e.g., **12**−**14**, demonstrate that the radical

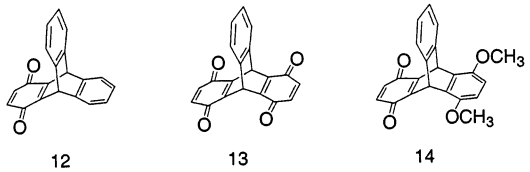

anion of **13** is localized on one ring, rather than spread over adjacent π-electron systems.[18] However, the presence of multiple quinone moieties significantly alters reduction potentials. The first reduction potential of the benzoquinone moiety of **12** is increased by 0.14 V upon introduction of the second quinone in **13**.[19] On the other hand, when one of the quinone moieties of **13** is reduced and protected as the dimethoxybenzene derivative as in **14**, the quinone first reduction potential is essentially identical to that of **12**.[20]

By analogy, the first reduction potential of the naphthoquinone moiety of **1** in the absence of prior reduction of the benzoquinones is expected to be higher than the −0.52 V potential measured for **4** by at least 0.14 V, yielding a potential ≥ -0.38 V. The potential could be higher than −0.38 V if the presence of two additional quinones has a greater effect than the presence of one. Thus, in Figure 4, the energy of $P^{\bullet+}-NQ^{\bullet-}-BQ_2$ is estimated as ≤ 1.31 eV above the ground state.

Electron-Transfer Pathways. The electron-transfer rate data gleaned from the transient absorption studies may be interpreted in terms of the elementary processes indicated in Figure 4. Relevant energies and rate constants are given in Table 2. For dyad **2** in benzonitrile, k_1, the rate constant for step 1 (Figure 4a), is 1.0×10^8 s^{-1} on the basis of the lifetime of ^{1}P in model porphyrin **11**. The rate constant for photoinduced electron transfer, 2.4×10^{10} s^{-1}, may be associated with k_2. Charge recombination of $P^{\bullet+}-NQ^{\bullet-}$ to the ground state, step 3, occurs with $k_3 \sim 3 \times 10^{12}$ s^{-1}.

Turning now to tetrad **1** (Figure 4b), the value of k_1 in benzonitrile may again be assigned as 1.0×10^8 s^{-1}. For the reasons explained above, charge recombination of $P^{\bullet+}-NQ-(BQ^{\bullet-}BQ)$ by step 6 is assigned a value of $k_6 = 1.9 \times 10^{10}$ s^{-1}. We cannot say with certainty whether this involves direct electron transfer from a benzoquinone to the porphyrin radical cation, or stepwise, endergonic formation of $P^{\bullet+}-NQ^{\bullet-}-BQ_2$ followed by rapid recombination of this species via step 3. The slow recombination of the final charge-separated state in tetrad **1** (1.9×10^{10} s^{-1}) relative to the recombination of $P^{\bullet+}-NQ^{\bullet-}$ in dyad **2** ($\sim 3 \times 10^{12}$ s^{-1}) is excellent evidence that the final state in **1** is indeed $P^{\bullet+}-NQ-(BQ^{\bullet-}BQ)$ rather than $P^{\bullet+}-NQ^{\bullet-}-BQ_2$. Recombination of $P^{\bullet+}-NQ^{\bullet-}$ and $P^{\bullet+}-NQ^{\bullet-}-BQ_2$ to the ground state would occur in the inverted region of the Marcus−Hush rate constant vs thermodynamic driving force relationship.[21,22] The driving force for recombination of $P^{\bullet+}-NQ^{\bullet-}-BQ_2$ would be less than that for recombination of $P^{\bullet+}-NQ^{\bullet-}$, because the electron withdrawing nature of the benzoquinone moieties would increase the reduction potential of the naphthoquinone in **1**, as discussed above. Thus, recombination of $P^{\bullet+}-NQ^{\bullet-}-BQ_2$ in **1** would be faster than recombination of $P^{\bullet+}-NQ^{\bullet-}$ in **2**. The fact that slower recombination is observed is only consistent with $P^{\bullet+}-NQ-(BQ^{\bullet-}BQ)$ as the final state.

To what elementary processes does the photoinduced electron-transfer rate constant of 8.3×10^{10} s^{-1} observed for **1** correspond? Clearly, it is made up of some combination of the rates of steps 2 and 4 in Figure 4b:

$$k_2 + 2k_4 = 8.3 \times 10^{10} \qquad (3)$$

If we were to assume that k_2 has the same value for dyad **2** and tetrad **1**, then k_4 would be 3.0×10^{10} s^{-1}. However, we know that k_2 in **1** must be larger than it is in **2**. This is the case because the naphthoquinone is a better electron acceptor in **1** than in **2** by ≥ 0.14 eV due to the presence of the benzoquinones, as discussed above. This increases the thermodynamic driving force for step 2 in **1**. As this electron transfer undoubtedly occurs in the "normal" region of the Marcus−Hush rate constant vs thermodynamic driving force relationship,[21,22] the driving force increase leads to a larger electron-transfer rate constant. A quantitative estimate of this increase may be made using the results of Joran et al., who have studied photoinduced electron transfer in porphyrin−quinone systems as a function of thermodynamic driving force.[23] Using their results for electron transfer in butyronitrile solvent, an increase in driving force of ≥ 0.14 eV in the appropriate range of free energy change values leads to a ≥ 4.8-fold increase in electron-transfer rate constant. This predicts that the rate constant for step 2 should increase from 2.4×10^{10} s^{-1} in **2** to $\geq 1.2 \times 10^{11}$ s^{-1} in **1**. This predicted rate constant is on the order of the value of 8.3×10^{10} s^{-1} measured for photoinduced electron transfer in **1**. On this basis, we assign the value of 8.3×10^{10} s^{-1} to k_2 in tetrad **1** (Figure 4b).

Assuming this interpretation to be correct, it is clear that photoinduced electron transfer in tetrad **1** proceeds mainly by a sequential, two-step mechanism. Photoinduced electron transfer from $^1P-NQ-BQ_2$ by step 2 yields $P^{\bullet+}-NQ^{\bullet-}-BQ_2$, which evolves by charge shift step 5 to give the final $P^{\bullet+}-NQ-(BQ^{\bullet-}BQ)$ charge-separated state. Although direct photoinduced electron transfer from the porphyrin first excited singlet state to a benzoquinone moiety (step 4) is thermodynamically allowable in **1**, it does not occur rapidly enough to have any detectable effects.

Although the above arguments suggest that photoinduced electron transfer from the porphyrin first excited singlet state of **1** directly to a benzoquinone moiety does not have to be invoked to explain the observed behavior, electron transfer to benzoquinones in related structures can be detected when no naphthoquinone acceptor is present. For example, in dichloromethane, photoinduced electron transfer from C−^{1}P−BQ in carotenoid (C) porphyrin quinone triad **15** occurs with a rate

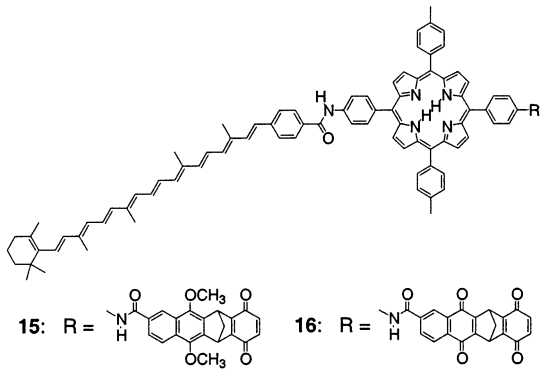

constant[12,24] of 9.6×10^8 s^{-1}. Under the same conditions, photoinduced electron transfer in C−P−NQ−BQ tetrad **16**, which includes a naphthoquinone intermediate electron acceptor, is much faster, with a rate constant[24] of 6.6×10^{10} s^{-1}.

Charge Recombination. Although photoinduced electron transfer in dyad **2** occurs efficiently to produce a high yield of the charge-separated state, the lifetime of that state is so short (~300 fs) that access to the stored energy via chemical reactions, coupling to electrodes, etc., would be difficult. In contrast, the multistep electron-transfer pathway illustrated for **1** in Figure 4b allows the formation of a much longer lived (52 ps) charge-separated state. This multistep electron-transfer strategy has been exploited in many other artificial photosynthetic systems.[1−10]

Yield of the Long-Lived Charge-Separated State. As mentioned earlier, the quantum yield of photoinduced electron transfer in **1** is essentially unity. However, because we were not able to distinguish spectroscopically between $P^{\bullet+}-NQ^{\bullet-}-BQ_2$ and $P^{\bullet+}-NQ-(BQ^{\bullet-}BQ)$, and because of the inverted kinetic situation found for **2**, which presumably occurs in **1** as well, we cannot determine the rate constant for step 5 in Figure 4b, or calculate the yield of $P^{\bullet+}-NQ-(BQ^{\bullet-}BQ)$ from kinetic parameters. We can roughly estimate the yield from the amplitude of the transient absorption of the porphyrin radical cation by comparing this amplitude with that of a porphyrin−fullerene dyad[25] having a quantum yield for charge separation of 1.0. The two solutions had the same absorbance at the pump wavelength of 648 nm. The comparison suggests that the yield of $P^{\bullet+}-NQ-(BQ^{\bullet-}BQ)$ is nearly quantitative, although a precise determination cannot be made because the porphyrin moieties in question differ somewhat, and this affects the shapes and intensities of their transient absorption spectra.

Given a two-step electron-transfer mechanism, the yield of $P^{\bullet+}-NQ-(BQ^{\bullet-}BQ)$ in **1** would necessarily be enhanced over that for a similar compound having only one benzoquinone moiety (analogous to tetrad **16**). This is because in **1** there are two charge-shift reactions (one to each benzoquinone) competing with charge recombination of the initial charge-separated state, rather than one. The two reactions operate in parallel to yield the final state. Of course, the degree of the enhancement will become smaller as the quantum yield approaches unity. Other examples of parallel multistep electron-transfer reactions that increase yields have been reported.[2]

Comparison with Other Systems. It is interesting to compare the results reported here for **1** and **2** with those recently reported for a series of porphyrin−quinone dyads and $P-BQ_a-BQ_b$ triads exemplified by **17** and **18**.[14] Time-resolved fluorescence studies of these molecules in dichloromethane show that the dyads exhibit two exponential decay components: a short lifetime (52 ps for **17**) corresponding to quenching of the porphyrin first excited singlet state by photoinduced electron transfer to the quinone, and a small amount of a long-lived component (7.7 ns for **17**) assigned to molecules in which the quinone has been adventitiously reduced to the hydroquinone. The triads, on the other hand, feature not only a short (20 ps for **18**) and a long-lived (7.5 ns for **18**) component, but also a decay component of intermediate lifetime (900 ps for **18**). In the triads, the short-lived component was assigned to photoinduced electron transfer to the quinone moiety nearest the porphyrin (Q_a), the intermediate lifetime to photoinduced electron transfer directly to the quinone farthest from the porphyrin (Q_b), and the long lifetime to porphyrin lacking quinone moieties.[14] This was taken as evidence for decay of the porphyrin first excited singlet states of the triads by direct photoinduced electron transfer to each of the two quinones, with no evidence for stepwise transfer. Clearly, this could only be the case if there are two conformational populations of quinones that do not interconvert on the fluorescence time scale—one with conformations favoring electron transfer to Q_a, and a second with conformations in which transfer to Q_a is slowed to the point that electron transfer to Q_b dominates. Otherwise, photoinduced electron transfer involving direct donation to both Q_a and Q_b would simply decrease the time constant for the single exponential decay of the porphyrin first excited singlet state, rather than give rise to two decay components. Thus, we feel that although direct electron transfer to both of the quinone moieties in these triads may in fact occur, the additional lifetimes observed are likely associated with impurities such as triads in which Q_a, but not Q_b, has been reduced to hydroquinone by adventitious reducing agents. Experience in many laboratories has shown that it is extremely difficult to prevent reduction of a small fraction of benzoquinone in such compounds under ambient conditions.

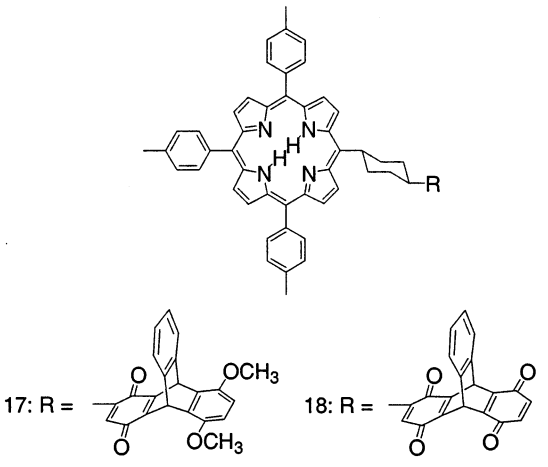

Conclusion

These results demonstrate that in benzonitrile, photoinduced electron transfer from ^1P-NQ in dyad **2** to yield $P^{\bullet+}-NQ^{\bullet-}$ occurs with a quantum yield of essentially unity but that the charge-separated state recombines to form the ground state extremely rapidly. On the other hand, photoinduced electron transfer in tetrad **1** yields $P^{\bullet+}-NQ^{\bullet-}-BQ_2$, which evolves by charge shift to give a final charge-separated state $P^{\bullet+}-NQ-(BQ^{\bullet-}BQ)$. The final state has a significantly longer lifetime than does $P^{\bullet+}-NQ^{\bullet-}$ in dyad **2**, demonstrating the use of a sequential two-step electron transfer to enhance charge separation lifetimes. Similar strategies are used in natural photosynthetic reaction centers. In addition, tetrad **1** demonstrates parallel multistep electron-transfer behavior. The initial $P^{\bullet+}-NQ^{\bullet-}-BQ_2$ state has two identical decay pathways leading to $P^{\bullet+}-NQ-(BQ^{\bullet-}BQ)$, both of which compete with the rapid charge recombination. The enhanced rate of photoinduced electron transfer observed for **1** relative to **2** is in accord with the expected increase in the first reduction potential of the naphthoquinone moiety resulting from interactions with the two benzoquiones. No contribution of direct electron transfer from the porphyrin first excited singlet state to a benzoquinone moiety is necessary to interpret the observations.

Experimental Section

Instrumental Techniques. All spectroscopic data were collected at room temperature. The ^1H NMR spectra were recorded on Varian Unity spectrometers at 300 or 500 MHz.

Samples were dissolved in $CDCl_3$ containing tetramethylsilane as an internal reference. Mass spectra were obtained on a Finnigan MAT model 312 spectrometer operating at 70 eV in EI mode. Other mass spectra were obtained on a Vestec Lasertec matrix-assisted laser desorption/ionization time-of-flight spectrometer (MALDI-TOF). Ultraviolet−visible ground-state absorption spectra were measured on a Shimadzu UV2100U UV−vis spectrometer.

Steady-state fluorescence emission spectra were measured using a Photon Technology International MP-1 spectrometer and corrected. Excitation was produced by a 75 W xenon lamp and single-grating monochromator. Fluorescence was detected at 90° to the excitation beam via a single grating monochromator and an R928 photomultiplier tube having S-20 spectral response and operating in the single photon counting mode.

Fluorescence decay measurements were performed on $\sim 1 \times 10^{-5}$ M solutions by the time-correlated single photon counting method. The excitation source was a cavity-dumped Coherent 700 dye laser pumped by a frequency-doubled Coherent Antares 76s Nd:YAG laser. Fluorescence emission was detected at a magic angle using a single grating monochromator and microchannel plate photomultiplier (Hamamatsu R2809U-11). The instrument response time was ca. 35−50 ps, as verified by scattering from Ludox AS-40. The spectrometer was controlled by software based on a LabView program from National Instruments.[26]

The femtosecond transient absorption apparatus consisted of a kilohertz pulsed laser source and a pump−probe optical setup, as previously described.[27,28] To determine the number of lifetime components in the transient absorption data, singular value decomposition analysis was performed and decay-associated spectra derived, as previously described.[27]

2-Carbomethoxy-7,10,15,18-tetramethoxy-6,11-dihydro-6,11-[1,2]benzenotetracen-5,12-quinone (4). To a 250-mL round-bottom flask containing 100 mL of 5 M lithium perchlorate ($LiClO_4$) in ethyl acetate was added 1,4,5,8-tetramethoxyanthracene[29] (512 mg, 1.72 mmol) and 2-carbomethoxy-5,8-naphthoquinone[30] (739 mg, 3.42 mmol). The reaction mixture was stirred and refluxed for 2 weeks. Ethyl acetate was added as needed to maintain volume. The reaction mixture was poured into 100 mL of water. The mixture was extracted with 250 mL of dichloromethane, which was then dried over sodium sulfate. After the solvent was distilled at reduced pressure, a dark purple residue remained. The residue was purified by column chromatography, using silica gel and eluting with a 3:1 mixture of dichloromethane and hexanes. Upon removal of the solvent, 399 mg of a red solid remained (45% yield). ^{1}H NMR (300 MHz, $CDCl_3$): δ 8.68 (1H, d, $J = 2$ Hz), 8.29 (1H, dd, $J = 8$ Hz, 2 Hz), 8.13 (1H, d, $J = 8$ Hz), 6.87 (1H, s), 6.86 (1H, s), 6.55 (4H, s), 3.96 (3H, s), 3.82 (12H, s). MS (EI): *m*/*z* 512 ($C_{30}H_{24}O_8^+$).

2-Carbomethoxy-5,7,10,12,15,18-hexamethoxy-6,11-dihydro-6,11-[1,2]benzenotetracene (5). The oxidized Diels−Alder adduct **4** (136 mg, 0.265 mmol) was suspended in 80 mL of tetrahydrofuran in a 200-mL round-bottom flask. Sodium dithionite (1.12 g) and 10 mL of water were added. The red suspension gradually became orange over 15 min. Two more portions of sodium dithionite (0.38 and 0.54 g) were added over 30 min. The reaction mixture was heated to 50 °C and two more portions of sodium dithionite (0.38 and 0.35 g) were added over 30 min. The reaction mixture gradually turned into an orange solution over the next 20 min. The reaction mixture was then heated to reflux, and 0.8 mL of dimethyl sulfate was added. Next, 25 mL of 10% aqueous potassium hydroxide was added dropwise through an addition funnel over 15 min. The reaction mixture gradually became yellow and was allowed to cool to room temperature. It was poured into 150 mL of 1 N HCl and extracted with chloroform. The organic layer was washed once with 10% sodium bicarbonate and then dried (sodium sulfate). The solvent was evaporated, leaving a yellow solid, which was purified on a silica gel column (1:9 ethyl acetate: dichloromethane) to give 81 mg of white solid **5** (56% yield). ^{1}H NMR (300 MHz, $CDCl_3$): δ 8.73 (1H, d, $J = 2$ Hz), 8.03 (1H, d, $J = 9$ Hz), 7.97 (1H, dd, $J = 9$ Hz, 2 Hz), 6.86 (2H, s), 6.56 (4H, s), 4.07 (3H, s), 4.04 (3H, s), 3.94 (3H, s), 3.85 (12H, s). MS (EI): *m*/*z* 542 ($C_{32}H_{30}O_8^+$).

2-Carboxy-5,7,10,12,15,18-hexamethoxy-6,11-dihydro-6,11-[1,2]benzenotetracene (6). Into a 200-mL round-bottom flask were added 63 mg of triquinone ester **5** (0.12 mmol) and 50 mL of a 1:1 mixture of tetrahydrofuran and methanol. To this was added 10 mL of 10% aqueous potassium hydroxide. The mixture was stirred at 50 °C for 24 h. After 50 mL of 1 N HCl was added, the mixture was extracted with dichloromethane. The organic layer was dried (sodium sulfate) and the solvent was distilled at reduced pressure, leaving a white solid, **6** (60.2 mg, 98% yield), which was used without further purification. ^{1}H NMR (300 MHz, $CDCl_3$): δ 8.81 (1H, d, $J = 1$ Hz), 8.06 (1H, d, $J = 9$ Hz), 8.00 (1H, dd, $J = 9$ Hz, 1 Hz), 6.87 (1H, s), 6.86 (1H, s), 6.57 (4H, s), 4.08 (3H, s), 4.04 (3H, s), 3.85 (12H, s). MS (EI): *m*/*z* 528 ($C_{31}H_{28}O_8^+$).

Porphyrin derivative 7. Acid **6** (92.4 mg, 0.175 mmol) was suspended in 20 mL of dichloromethane and 2 mL of pyridine. To the white suspension was added 0.6 mL (8.2 mmol) of thionyl chloride. The dichloromethane and excess thionyl chloride were removed under vacuum, leaving a yellow residue. To the residue were added 10 mL of dichloromethane and 2 mL of pyridine. Porphyrin **10**[3] (126 mg, 0.164 mmol) dissolved in 20 mL of dichloromethane was added. The reaction mixture was stirred under argon at room temperature for 46 h. The reaction mixture was quenched with 100 mL of 10% aqueous sodium bicarbonate and extracted with dichloromethane. The dichloromethane solution was dried (sodium sulfate) and evaporated, leaving a purple solid. The solid was purified on a silica gel column (5% methanol in dichloromethane as eluant), resulting in the desired tetrad, **7** (106 mg, 56% yield). ^{1}H NMR (500 MHz, $CDCl_3$): δ 8.88 (6H, brs), 8.78 (2H, m), 8.66 (1H, d, $J = 2$ Hz), 8.61 (1H, brs), 8.30 (1H, brs), 8.25 (2H, d, $J = 8$ Hz), 8.23 (2H,d, $J = 9$ Hz), 8.19 (1H, d, $J = 9$ Hz), 8.09 (6H, d, $J = 8$ Hz), 8.03 (1H, dd, $J = 9$ Hz, 2 Hz), 7.97 (2H, d, $J = 9$ Hz), 7.55 (4H, d, $J = 8$ Hz), 6.92 (1H, s), 6.91 (1H, s), 6.60 (4H, s), 4.17 (3H, s), 4.10 (3H, s), 3.88 (12H, s), 2.70 (6H, s), −2.78 (2H, brs). MS (MALDI-TOF): *m*/*z* 1279.2 ($C_{79}H_{61}F_3N_6O_8^+$).

Porphyrin derivative 8. Compound **7** (106 mg, 0.083 mmol) was suspended in 40 mL of tetrahydrofuran and 20 mL of methanol. Aqueous potassium hydroxide (10%, 3 mL) was added, and the reaction mixture was stirred at room temperature for 90 h. Water (100 mL) was added, followed by extraction with dichloromethane. The dichloromethane was dried (sodium sulfate) and evaporated, leaving a purple solid. Some starting material was still present and was separated by column chromatography using silica gel and 3% ethyl acetate in dichloromethane as the eluant. The unreacted starting material was subjected to the same reaction conditions for 4 days. After an identical workup, no starting material remained. The product was the desired porphyrin amine **8** (94.8 mg, 97% yield). ^{1}H NMR (300 MHz, $CDCl_3$): δ 8.92, (2H, d, $J = 5$ Hz), 8.86 (6H, m), 8.67 (1H, d, $J = 2$ Hz), 8.30 (1H, brs), 8.23 (2H, d,

J = 9 Hz), 8.19 (2H, d, J = 8 Hz), 8.10 (4H, d, J = 8 Hz), 8.08 (2H, d, J = 8 Hz), 8.04 (1H, dd, J = 8 Hz), 7.99 (2H, d, J = 8 Hz), 7.56 (4H, d, J = 8 Hz), 7.06 (2H, d, J = 9 Hz), 6.93 (1H, s, H6), 6.92 (1H, s), 6.60 (4H, s), 4.18 (3H, s), 4.11 (3H, s), 3.89 (12H, s), 2.71 (6H, s), −2.74 (2H, brs). MS (MALDI-TOF): m/z 1184.4 ($C_{77}H_{62}N_6O_7^+$).

Tetrad 1. This reaction was performed under subdued lighting. Compound **8** (94.8 mg, 0.087 mmol) was suspended in 50 mL of dichloromethane in a 200-mL single-neck round-bottom flask. After the flask was placed in a dry ice/acetone bath, 5 mL of 1.0 M boron tribromide in dichloromethane was added, turning the reaction mixture green immediately. The mixture was stirred in the dry ice bath for 30 min and then at room temperature for 2 h. Aqueous sodium bicarbonate (10%, 100 mL) was added. The mixture was extracted with dichloromethane and then washed twice with water and once with 0.1 M aqueous potassium periodate. The organic phase was dried (sodium sulfate) and evaporated, leaving a purple solid. The solid was purified by chromatography on silica gel (10% ethyl acetate in dichloromethane) to yield 52.3 mg (60%) of **1**. ^{1}H NMR (500 MHz, $CDCl_3$): δ 8.92, (2H, d, J = 4 Hz), 8.85 (6H, m), 8.64 (1H, d, J = 2 Hz), 8.43 (1H, dd, J = 8 Hz, 2 Hz), 8.28 (2H, d, J = 8 Hz), 8.24 (2H, d, J = 9 Hz), 8.09 (4H, d, J = 8 Hz), 8.05 (1H, d, J = 8 Hz), 7.99 (2H, d, J = 9 Hz), 7.55 (4H, d, J = 8 Hz), 7.06 (2H, d, J = 8 Hz), 6.95 (1H, s), 6.86 (1H, s), 6.71 (4H, s), 4.06 (2H, brs), 2.70 (6H, s), −2.76 (2H, brs). MS (MALDI-TOF): m/z 1094.7 ($C_{71}H_{44}N_6O_7^+$).

2-Carboxy-7,10,15,18-tetramethoxy-6,11-dihydro-6,11-[1,2]benzenotetracen-5,12-quinone (9). Ester **4** (47 mg, 0.092 mmol) and 98 mg of sodium acetate (1.19 mmol) were added to a 200-mL round-bottom flask. A solution of 203 mg of lithium iodide (1.52 mmol) in 30 mL of DMF was then added. Upon heating, all of the solids dissolved, giving an orange solution, which was refluxed for 24 h. An additional 300 mg of LiI was added, and the reaction mixture was refluxed for an additional 6 h. The reaction mixture was then cooled to room temperature, poured into 100 mL of water, and extracted with dichloromethane. The organic phase was dried over magnesium sulfate and the solvent was stripped, leaving a tan residue, which was purified by column chromatography (silica gel, 20% methanol in dichloromethane) to give 30 mg of tan solid, **9** (65% yield). ^{1}H NMR (300 MHz, $CDCl_3$): δ 8.73, (1H, brs), 8.32 (1H, d, J = 8 Hz), 8.15 (1H, d, J = 8 Hz), 6.88 (1H, s), 6.86 (1H, s), 6.55 (4H, s), 3.83 (12H, s). MS (MALDI-TOF): m/z 500.4 ($C_{29}H_{22}O_8^+ + 2$).

Dyad 2. To a 200-mL, single-neck round-bottom flask was added 23 mg of **9** (0.046 mmol) followed by 20 mL of dichloromethane and 2 mL of dry pyridine. The reaction mixture was purged with argon and 0.65 mL of thionyl chloride was added. The reaction mixture immediately turned from a tan suspension to an orange solution. The solvent was distilled under vacuum, leaving an orange residue, which was dissoslved in dichloromethane and transferred to a 25-mL addition funnel. The acid chloride solution was added dropwise over 15 min under subdued lighting to a 100-mL round-bottom flask containing 39 mg of 5,15-diamino-10,20-bis(4-methylphenyl)-porphyrin (0.058 mmol),[31] 50 mL of dichloromethane, and 2 mL of dry pyridine. The reaction mixture was stirred at room temperature for 4 h and then quenched with 100 mL of 10% aqueous $NaHCO_3$. The mixture was then extracted with dichloromethane and dried over sodium sulfate. After removal of the solvent, a purple residue was left, which was purified by chromatography on silica gel (5% ethyl acetate in dichloromethane) to yield 27.5 mg (52% yield) of **2** as a purple solid. ^{1}H NMR (300 MHz, $CDCl_3$): δ 8.92, (2H, d, J = 5 Hz), 8.85 (6H, m), 8.62 (1H, d, J = 2 Hz), 8.38 (1H, dd, J = 8 Hz, 2 Hz), 8.27 (1H, d, J = 8 Hz), 8.21 (2H, d, J = 8 Hz), 8.09 (4H, d, J = 8 Hz), 8.03 (2H, d, J = 9 Hz), 7.99 (2H, d, J = 9 Hz), 7.55 (4H, d, J = 8 Hz,), 7.05 (2H, d, J = 8 Hz), 6.93 (1H, s), 6.92 (1H, s), 6.58 (4H, s), 3.87 (12H, s), 3.64 (1H, brs), 2.71 (6H, s), −2.75 (2H, brs). MS (MALDI-TOF): m/z 1153.3 ($C_{75}H_{56}N_6O_7^+$).

2-Carbomethoxy-6,11-dihydro-6,11-[1,2]benzenotetracen-5,7,10,12,15,18-triquinone (3). The Diels−Alder adduct **4** (42.5 mg, 0.088 mmol) was suspended in 50 mL of acetonitrile in a 500-mL round-bottom flask. Ceric ammonium nitrate (CAN) (7.15 g, 13.0 mmol) was dissolved in 30 mL of water in a 125-mL addition funnel, and added dropwise to the flask. The reaction mixture changed from a red suspension to a yellow-orange solution after approximately half of the CAN solution was added. When addition was complete, the reaction mixture was diluted with 100 mL of water and extracted with dichloromethane. The organic extract was washed once with 10% aqueous potassium periodate and dried over sodium sulfate. After the solvent was distilled at reduced pressure, a yellow residue remained, which was purified over a short silica gel column (5% acetone in dichloromethane). Removal of the solvent left 19 mg (51% yield) of **3**. ^{1}H NMR (300 MHz, $CDCl_3$): δ 8.67 (1H, d, J = 2 Hz), 8.34 (1H, dd, J = 8 Hz, 2 Hz), 8.14 (1H, d, J = 8 Hz), 6.78 (1H, s), 6.77 (1H, s), 6.70 (4H, s), 3.97 (3H, s). MS (MALDI-TOF): m/z 453.1 ($C_{26}H_{12}O_8^+ + 1$).

Acknowledgment. This work was supported by a grant from the U. S. Department of Energy (DE-FG03-93ER14404). This is publication 558 from the ASU Center for the Study of Early Events in Photosynthesis.

References and Notes

(1) Gust, D.; Moore, T. A.; Moore, A. L. *Acc. Chem. Res.* **2001**, *34*, 40−48.

(2) Gust, D.; Moore, T. A. In *The Porphyrin Handbook*; Kadish, K. M., Smith, K. M., Guilard, R., Eds.; Academic Press: New York, 2000; pp 153−190.

(3) Gust, D.; Moore, T. A.; Moore, A. L.; Macpherson, A. N.; Lopez, A.; DeGraziano, J. M.; Gouni, I.; Bittersmann, E.; Seely, G. R.; Gao, F.; Nieman, R. A.; Ma, X. C.; Demanche, L. J.; Luttrull, D. K.; Lee, S.-J.; Kerrigan, P. K. *J. Am. Chem. Soc.* **1993**, *115*, 11141−11152.

(4) Gust, D.; Moore, T. A. *Adv. Photochem.* **1991**, *16*, 1−65.

(5) Wasielewski, M. R. *Chem. Rev.* **1992**, *92*, 435−461.

(6) Bixon, M.; Fajer, J.; Feher, G.; Freed, J. H.; Gamliel, D.; Hoff, A. J.; Levanon, H.; Möbius, K.; Nechushtai, R.; Norris, J. R.; Scherz, A.; Sessler, J. L.; Stehlik, D. *Isr. J. Chem.* **1992**, *32*, 449−455.

(7) Asahi, T.; Ohkouchi, M.; Matsusaka, R.; Mataga, N.; Zhang, R. P.; Osuka, A.; Maruyama, K. *J. Am. Chem. Soc.* **1993**, *115*, 5665−5674.

(8) Connolly, J. S.; Bolton, J. R. In *Photoinduced Electron Transfer, Part D*; Fox, M. A., Chanon, M., Eds. Elsevier: Amsterdam, 1988; pp 303−393.

(9) Sakata, Y.; Imahori, H.; Tsue, H.; Higashida, S.; Akiyama, T.; Yoshizawa, E.; Aoki, M.; Yamada, K.; Hagiwara, K.; Taniguchi, S.; Okada, T. *Pure Appl. Chem.* **1997**, *69*, 1951−1956.

(10) Imahori, H.; Sakata, Y. *Adv. Mater.* **1997**, *9*, 537−546.

(11) Nishitani, S.; Kurata, N.; Sakata, Y.; Misumi, S.; Karen, A.; Okada, T.; Mataga, N. *J. Am. Chem. Soc.* **1983**, *105*, 7771−7772.

(12) Gust, D.; Moore, T. A.; Moore, A. L.; Barrett, D.; Harding, L. O.; Makings, L. R.; Liddell, P. A.; de Schryver, F. C.; Van der Auweraer, M.; Bensasson, R. V.; Rougée, M. *J. Am. Chem. Soc.* **1988**, *110*, 321−323.

(13) Gust, D.; Moore, T. A.; Moore, A. L.; Lee, S.-J.; Bittersmann, E.; Luttrull, D. K.; Rehms, A. A.; DeGraziano, J. M.; Ma, X. C.; Gao, F.; Belford, R. E.; Trier, T. T. *Science* **1990**, *248*, 199−201.

(14) Korth, O.; Wiehe, A.; Kurreck, H.; Röder, B. *Chem. Phys.* **1999**, *246*, 363−372.

(15) Kuciauskas, D.; Liddell, P. A.; Hung, S.-C.; Lin, S.; Stone, S.; Seely, G. R.; Moore, A. L.; Moore, T. A.; Gust, D. *J. Phys. Chem.* **1997**, *101*, 429−440.

(16) Gasyna, Z.; Browett, W. R.; Stillman, M. J. *Inorg. Chem.* **1985**, *24*, 2440−2447.
(17) Hung, S.-C.; Lin, S.; Macpherson, A. N.; DeGraziano, J. M.; Kerrigan, P. K.; Liddell, P. A.; Moore, A. L.; Moore, T. A.; Gust, D. *J. Photochem. Photobiol. A* **1994**, *77*, 207−216.
(18) Russell, G. A.; Suleman, N. K. *J. Am. Chem. Soc.* **1981**, *103*, 1560−1561.
(19) Iwamura, H.; Makino, K. *Chem. Commun.* **1978**, 720−721.
(20) Yamamura, K.; Miyake, H.; Himeno, S.; Inagaki, S.; Nakasuji, K.; Murata, I. *Chem. Lett.* **1988**, 1819−1822.
(21) Marcus, R. A. *J. Chem. Phys.* **1956**, *24*, 966−978.
(22) Marcus, R. A. *Pure Appl. Chem.* **1997**, *69*, 13−29.
(23) Joran, A. D.; Leland, B. A.; Felker, P. M.; Zewail, A. H.; Hopfield, J. J.; Dervan, P. B. *Nature* **1987**, *327*, 508−511.
(24) Harding, L. O. G. Preparation and photochemistry of photosynthesis model systems. Ph.D. Dissertation, Arizona State University, Tempe, AZ, 1989.
(25) Kodis, G.; Liddell, P. A.; de la Garza, L.; Clausen, P. C.; Lindsey, J. S.; Moore, A. L.; Moore, T. A.; Gust, D. *J. Phys. Chem. A* **2002**, *106*, 2036−2048.
(26) Gust, D.; Moore, T. A.; Luttrull, D. K.; Seely, G. R.; Bittersmann, E.; Bensasson, R. V.; Rougée, M.; Land, E. J.; de Schryver, F. C.; Van der Auweraer, M. *Photochem. Photobiol.* **1990**, *51*, 419−426.
(27) Liddell, P. A.; Kodis, G.; de la Garza, L.; Bahr, J. L.; Moore, A. L.; Moore, T. A.; Gust, D. *Helv. Chim. Acta* **2001**, *84*, 2765−2783.
(28) Freiberg, A.; Timpmann, K.; Lin, S.; Woodbury, N. W. *J. Phys. Chem. B* **1998**, *102*, 10974−10982.
(29) Fitzgerald, J. J.; Drysdale, N. E.; Olofson, R. A. *Synth. Commun.* **1992**, *22*, 1807−1812.
(30) Gust, D.; Moore, T. A.; Moore, A. L.; Seely, G. R.; Liddell, P. A.; Barrett, D.; Harding, L. O.; Ma, X. C.; Lee, S.-J.; Gao, F. *Tetrahedron* **1989**, *45*, 4867−4891.
(31) Gust, D.; Moore, T. A.; Moore, A. L.; Liddell, P. A. *Methods Enzymol.* **1992**, *213*, 87−100.